https://doi.org/10.5194/egusphere-2025-6499
Preprint. Discussion started: 13 January 2026
© Author(s) 2026. CC BY 4.0 License.

Spatiotemporal reorganization of global earthquake disaster impacts within coupled human-Earth systems

Zekang Zhang[1], Yingqiao Qiu[2,3], Yanjun Ye[1], and Chaoran Xuan[1]

[1]School of Earth Science and Engineering, Hebei University of Engineering, Handan 056038, China.
[2]Hebei Key Laboratory of Agricultural Water-Saving, Center for Agricultural Resources Research, Institute of Genetics and Developmental Biology, Chinese Academy of Sciences, Shijiazhuang 050022, China.
[3]School of Advanced Agricultural Sciences, University of Chinese Academy of Sciences, Beijing 100049, China.

Correspondence: Yanjun Ye (yeyanjun@hebeu.edu.cn)

Abstract. Understanding how earthquake disaster impacts reorganize across space and time is essential for interpreting seismic hazards within coupled human-earth systems. Using global disaster records from EM-DAT spanning 1980–2024, this study examines multi-scale spatiotemporal patterns of earthquake disaster impacts and their socio-environmental associations at global and national scales. Temporal analyses show a pronounced decoupling between seismic occurrence and disaster consequences: while earthquake frequency, exposed population, and cumulative economic losses increased overall, mortality rates declined markedly after the early 2000s. Spatial analyses reveal strong heterogeneity across continents, countries, and major tectonic plates. Asia accounts for a substantial share of global earthquake occurrences, affected populations, fatalities, and economic losses, yet national-level impacts vary considerably even under comparable tectonic settings. Standard deviation ellipse and centroid analyses further indicate an eastward to southeastward migration of the global earthquake disaster centroid over time, accompanied by relatively stable orientation and a modest contraction in spatial dispersion. To explore factors associated with national differences in fatalities, a Geographical Detector model is applied using cumulative fatalities as the dependent variable and a set of natural, climatic, socioeconomic, governance, infrastructure, and health-related variables as explanatory factors. Results show that population density and development- and governance-related indicators exhibit relatively high explanatory power, while interactions among factors generally strengthen spatial associations through bilinear or nonlinear enhancement. Overall, the findings suggest that global disparities in earthquake disaster impacts reflect the spatial co-configuration of hazard exposure, development conditions, and institutional capacity, contributing to a system-level understanding of how seismic disaster impacts evolve within coupled human-Earth systems.

1 Introduction

Earthquake disasters remain among the most destructive natural hazards worldwide, causing profound human, economic, and infrastructural losses each year (United Nations Office for Disaster Risk Reduction (UNDRR), 2023; Daniell et al., 2017). Despite notable advances in seismology, engineering design, and emergency response systems, global earthquake losses have not declined uniformly. Instead, rapid urban expansion, population concentration in seismic belts, and intensified development in tectonically active landscapes continue to elevate exposure and reinforce disaster vulnerability (Cutter, 2021; Aksha and

https://doi.org/10.5194/egusphere-2025-6499
Preprint. Discussion started: 13 January 2026
© Author(s) 2026. CC BY 4.0 License.

Khanal, 2019; Düzgün et al., 2023). This persistent rise in disaster impacts—despite improved monitoring and hazard science—illustrates a central paradox in contemporary earthquake risk: disasters increasingly emerge from the interaction between geophysical processes and evolving social–environmental conditions, with disaster risk becoming most visible through its realized impacts on populations and economies.

A human–environment systems perspective, widely adopted in disaster risk research, is essential for understanding these patterns because it situates earthquakes within the broader spatial processes that shape risk production (Gall et al., 2011; Lee et al., 2022). Geophysically, seismic hazards are structured by plate interactions, strain accumulation, and lithospheric deformation, forming persistent seismic belts such as the Pacific Ring of Fire and the Alpine–Himalayan arc (Bird, 2003a; Kagan and Jackson, 2016). Yet similar earthquakes often produce vastly different outcomes depending on demographic exposure, infrastructure quality, governance effectiveness, and environmental fragility (Anbarci et al., 2005; Keefer et al., 2011; Wyss et al., 2023). These disparities underscore a growing recognition that earthquake disasters arise not solely from tectonic forces, but from the coupled operation of natural hazards and socially mediated vulnerability across space (Cohen and Werker, 2008; Reid, 2013; Ismail-Zadeh, 2024).

Decades of empirical research highlight the importance of governance, inequality, institutional capacity, and land-use change in shaping disaster risk. Weak governance and corruption undermine building-code enforcement and response capacity, significantly amplifying earthquake mortality (Escaleras et al., 2007; Anbarci et al., 2005). Health system capacity and social capital influence post-disaster survival, particularly in high-density or resource-constrained regions (Flanagan et al., 2011). Environmental degradation—through deforestation, unregulated construction, and slope instability—magnifies secondary hazards such as landslides and debris flows (Cannon et al., 2003; De Ruiter et al., 2021). Together, these findings reinforce that earthquake disaster impacts reflect interacting natural, demographic, environmental, and governance processes within coupled human–environment systems (Lapietra et al., 2024).

Despite substantial progress in regional seismic hazard studies, global-scale analyses of earthquake disasters impacts, as distinct from seismicity alone, remain limited. Most global assessments rely on instrumental catalogs to evaluate earthquake occurrence, magnitude–frequency patterns, or aftershock clustering (Zaliapin and Ben-Zion, 2013; Kagan and Jackson, 2016). While crucial for characterizing physical processes, these studies do not explain why comparable earthquakes generate disproportionate losses across countries (Noy, 2016; Li et al., 2021; Guo et al., 2020). Recent global models of seismic exposure and vulnerability (Xofi et al., 2022) represent important advances but underrepresent governance, environmental change, and socio-economic inequality-factors identified by the Sendai Framework as root causes of escalating disaster risk (United Nations Office for Disaster Risk Reduction (UNDRR), 2023).

Moreover, the interaction effects among multiple drivers remain poorly understood at the global scale. Traditional regression approaches frequently assume linearity and overlook spatial stratification, non-linear amplification, and synergistic interactions, such as those between population density and governance quality or between basic public infrastructure, precipitation, and topography (Wang et al., 2010; Hu et al., 2011; Ansari et al., 2025). Yet multi-factor interactions increasingly determine where disaster hotspots emerge within rapidly changing socio-ecological systems (Burton, 2015; Aksha and Khanal, 2019). Address-

https://doi.org/10.5194/egusphere-2025-6499
Preprint. Discussion started: 13 January 2026
© Author(s) 2026. CC BY 4.0 License.

ing these analytical limitations requires tools capable of detecting spatial heterogeneity and quantifying both independent and interactive effects within complex, coupled systems.

To address these gaps, this study integrates EM-DAT global disaster records (1980–2024), GIS-based spatial analysis, and the Geographical Detector model to examine the spatiotemporal dynamics and associated drivers of earthquake disaster impacts at the global scale. Specifically, we address four interrelated scientific questions:

(1) How have global earthquake disasters evolved over time? We analyze long-term temporal trends in earthquake frequency, mortality, population affected, and economic losses.

(2) How do seismic disaster patterns vary spatially across continents, countries, and tectonic plates?

(3) How have global and plate-level seismic disaster hotspots reorganized over time, as reflected in centroid migration and directional patterns?

(4) Which natural, demographic, environmental, and governance factors—independently and interactively—shape global earthquake fatalities?

By situating seismic disasters within a multi-scale disaster risk perspective, this study provides a globally comparable assessment of earthquake disaster patterns over four decades, clarifies the spatial processes underlying disaster reorganization, and identifies priority regions where governance, healthcare, and land-use interventions can most effectively reduce seismic risk.

2 Data sources and processing

2.1 Data sources

This study used earthquake disaster records from the Emergency Events Database (EM-DAT), covering reported events with magnitudes ranging from 3.0 to 9.5 during the period 1980-2024 (CRED, 2024). EM-DAT is widely adopted in global disaster risk research because it systematically documents disaster impacts—including fatalities, affected populations, and economic losses—rather than focusing solely on physical seismicity, and has been extensively used in the international community (Rosvold and Buhaug, 2021; Peduzzi and Herold, 2005). The global national administrative boundaries data were from the Resource and Environmental Sciences Data Platform (Resource and Environmental Science Data Platform, 2024), and the plate boundary data were from the global plate boundary dataset (Bird, 2003b). To enhance data consistency, all EM-DAT earthquake disaster entries from 1980 to 2024 were extracted using the disaster subtype “Earthquake” and cross-checked to remove duplicate entries and records with incomplete impact information.. To improve temporal comparability, reported economic losses were converted to constant 2020 USD using World Bank deflators, thereby reducing the influence of inflation and interannual reporting inconsistencies.

https://doi.org/10.5194/egusphere-2025-6499
Preprint. Discussion started: 13 January 2026
© Author(s) 2026. CC BY 4.0 License.

2.2 Data processing

The EM-DAT database provides information including occurrence time, epicenter coordinates (latitude and longitude), affected countries (with ISO codes), affected population, fatalities, and economic losses. Based on these raw records, we constructed a harmonized national-level dataset through spatial matching and attribute aggregation. For each country, the following indicators were calculated: cumulative earthquake frequency, cumulative fatalities, cumulative affected population, and cumulative economic losses. To better capture disaster severity and normalized impacts, four per-event indicators were further derived: (1) Average number of affected people per event, (2) Average fatalities per event, (3) Average economic loss per event, and (4) Mortality rate (defined as fatalities relative to affected population). Together, these indicators form eight complementary impact-related metrics describing earthquake disaster outcomes at the national scale, capturing both aggregate burden and per-event intensity. Spatial linkage was performed using country ISO codes to ensure consistency across administrative, tectonic, and socio-environmental datasets.

3 Methods

3.1 Temporal variability analysis method

To characterize the temporal evolution of major global earthquake disasters from 1980 to 2024, with an emphasis on disaster impacts rather than seismic activity alone,, linear regression and the Mann-Kendall (MK) trend test were employed. These methods are widely applied in disaster risk and climate-related research to identify long-term trends in impact-related indicators under non-normal distributions and reporting uncertainty (Wang et al., 2021). The MK test, a non-parametric approach robust to outliers and missing values, was used to evaluate monotonic trends in eight earthquake disaster indicators, including frequency, fatalities, affected population, and economic losses. The MK statistic S was computed following standard procedures, as follows:

$$S = \sum_{i=1}^{n-1} \sum_{j=i+1}^{n} \text{sign}(x_j - x_i) \tag{1}$$

Where x_i and x_j represent two observations in the time series. The sign function returns 1, 0, or -1 depending on whether the difference is positive, zero, or negative.

The standardized Z-value was then derived to assess trend significance:

$$Z = \begin{cases} \frac{S-1}{\sqrt{\frac{n(n-1)(2n+5)}{18}}} & \text{if } S > 0 \\ 0 & \text{if } S = 0 \\ \frac{S+1}{\sqrt{\frac{n(n-1)(2n+5)}{18}}} & \text{if } S < 0 \end{cases} \tag{2}$$

https://doi.org/10.5194/egusphere-2025-6499
Preprint. Discussion started: 13 January 2026
© Author(s) 2026. CC BY 4.0 License.

A positive Z-value indicates an upward trend, while a negative value indicates a downward trend. Significance thresholds were set at $|Z|$ = 1.28 (90%), 1.64 (95%), and 2.33 (99%) (Casella and Berger, 2002). By combining linear regression slopes with MK significance testing, this approach captures both the magnitude and robustness of long-term changes in earthquake disaster impacts.

3.2 Spatial variability analysis method

3.2.1 Standard deviation ellipse (SDE)

Standard Deviation Ellipse (SDE) is widely used to quantify the directional tendency and dispersion of geographic phenomena (Wu et al., 2021; Xiong et al., 2019). In the context of disaster risk research, SDE provides an effective means to identify large-scale spatial reorganization and directional shifts of hazard impacts over time. In this study, the SDE method was applied to analyze the directional pattern and spatial concentration of global earthquake disaster events. The SDE is defined by three parameters: (1) rotation angle (θ), (2) standard deviation along the major axis (δ_x), and (3) standard deviation along the minor axis (δ_y). The relative coordinates of each point with respect to the regional centroid were computed as follows:

$$\widetilde{x} = (x_i - \bar{x}), \quad \widetilde{y} = (y_i - \bar{y}) \tag{3}$$

Where ($\bar{x}$, $\bar{y}$) represents the spatial mean center of all earthquake events. All events were assigned equal weights to ensure consistency with an impact-oriented spatial representation.

The rotation angle is defined as the clockwise angle between the positive north direction and the major axis of the ellipse, capturing the dominant spatial orientation of earthquake distribution. The tangent of the rotation angle θ was computed as:

$$\tan\theta = \frac{\sum_{i=1}^{n} W_i^2\widetilde{x}_i^2 - \sum_{i=1}^{n} W_i^2\widetilde{y}_i^2 + \sqrt{\left(\sum_{i=1}^{n} W_i^2\widetilde{x}_i^2 - \sum_{i=1}^{n} W_i^2\widetilde{y}_i^2\right)^2 + 4\left(\sum_{i=1}^{n} W_i^2\widetilde{x}_i^2\widetilde{y}_i^2\right)^2}}{2\sum_{i=1}^{n} W_i^2\widetilde{x}_i\widetilde{y}_i} \tag{4}$$

δ_x and δ_y denote the semi-major axis and semi-minor axis of the SDE:

$$\delta_x = \sqrt{\frac{\sum_{i=1}^{n}(W_i\bar{x}_i\cos\theta - W_i\bar{y}_i\sin\theta)^2}{\sum_{i=1}^{n} W_i^2}}, \quad \delta_y = \sqrt{\frac{\sum_{i=1}^{n}(W_i\bar{x}_i\sin\theta - W_i\bar{y}_i\cos\theta)^2}{\sum_{i=1}^{n} W_i^2}} \tag{5}$$

where δ_x major and δ_y minor denote the semi-major and semi-minor axes of the SDE. A larger contrast between the two axes indicates stronger directional structure, while changes in the minor axis reflect variations in spatial dispersion of disaster impacts.

3.2.2 Geometric centroid shift analysis

Geometric centroid shift analysis serves as a robust method for investigating the spatiotemporal evolution of geographic phenomena. In disaster studies, centroid migration offers an intuitive metric for tracking the relocation of impact concentration

https://doi.org/10.5194/egusphere-2025-6499
Preprint. Discussion started: 13 January 2026
© Author(s) 2026. CC BY 4.0 License.

zones over time. In this study, we leverage the gravity model to quantify the dynamics of the Geometric centroid of global seismic disasters. The three elements to be calculated are the X and Y coordinates of the Geometric centroid of the global seismic hazard and the distance moved by the Geometric Centroid, and the longitude and latitude of the Geometric Centroid of the seismic hazard, respectively. The calculation formulas are as follows:

$$\bar{X} = \frac{\sum_{i=1}^{n} W_i \times X_i}{\sum_{i=1}^{n} W_i}, \quad \bar{Y} = \frac{\sum_{i=1}^{n} W_i \times Y_i}{\sum_{i=1}^{n} W_i} \tag{6}$$

Where n is the number of disasters; i is the disaster number; X_i and Y_i are the longitude and latitude of the i seismic disaster, respectively; W_i is the weight, where all weights were set to 1 to reflect equal contribution of each event.

The Geometric Centroid shift distance D is calculated by the formula:

$$D = C\sqrt{\left(\bar{X}_2 - \bar{X}_1\right)^2 + \left(\bar{Y}_2 - \bar{Y}_1\right)^2} \tag{7}$$

Where C is a constant used to convert geographic coordinates to plane distances, ensuring comparability across global scales. Combined with SDE results, centroid shift analysis enables joint interpretation of spatial relocation and dispersion dynamics of earthquake disaster impacts.

3.3 Geographical detector

3.3.1 Single-factor detector

The Geographical Detector model (Geodetector) is a statistical method grounded in spatial stratification heterogeneity theory, designed to quantify the influence intensity of different factors on geographical phenomena and to reveal the underlying mechanisms driving spatial heterogeneity (Wang et al., 2010). Because it does not assume linearity or normality, the method is well suited for analyzing disaster impacts shaped by coupled natural and social processes. In this study, the factor detector was applied to assess the independent spatial explanatory power of multiple natural, socioeconomic, governance, infrastructure, and health-related factors on cumulative earthquake fatalities at the national scale. Explanatory strength was quantified using the q-statistic, which ranges from 0 to 1, with higher values indicating stronger spatial explanatory ability (Wang et al., 2016). The formula is as follows:

$$q = 1 - \frac{\sum_{h=1}^{L} N_h \sigma_h^2}{N\sigma^2} \tag{8}$$

Where q denotes the explanatory power quantifying the extent to which the independent variable X accounts for the spatial heterogeneity of the dependent variable Y, with a value range of [0,1]. L represents the number of strata, defined by the categorization of the independent variable X based on its attribute values. N_h denotes the number of samples within the h-th stratum, and σ_h^2 represents the variance of the h-th stratum, reflecting the dispersion degree of the dependent variable Y within the h-th category.

https://doi.org/10.5194/egusphere-2025-6499
Preprint. Discussion started: 13 January 2026
© Author(s) 2026. CC BY 4.0 License.

3.3.2 Interaction detector

To investigate the interaction effects between driving factors, the interaction detector was applied to calculate the joint explanatory power of two factors and determine their interaction type. The formula is as follows:

$$q(X_1 \cap X_2) = 1 - \frac{\sum_{h=1}^{L_{12}} N_{h12}\sigma_{h12}^2}{N\sigma^2} \tag{9}$$

Where $q(X_1 \cap X_2)$ denotes the interaction explanatory power, measuring the joint influence of factors X_1 and X_2 on Y. L_{12} represents the number of joint strata formed by the overlay of factors X_1 and X_2. h_{12} is the joint stratum index, indicating the h_{12}-th combined category. N_{h12} denotes the sample size in the joint stratum, i.e., the number of observations in the h_{12}-th combination. σ_{h12}^2 represents the variance of Y that joint stratum. Based on the comparison between $q(X_1 \cap X_2)$ and the individual q-values of X_1 and X_2, factor interactions can be identified as independent, bilinear enhancement ($q(X_1 \cap X_2) > \max(q_1, q_2)$), or nonlinear enhancement ($q(X_1 \cap X_2) > q_1 + q_2$). By comparing interaction q-values with individual q-values, interactions were classified as independent, bilinear enhancement, or nonlinear enhancement. This analysis characterizes statistical associations arising from the spatial co-occurrence of exposure, vulnerability, and institutional conditions, without implying causal relationships.

4 Spatiotemporal characteristics analysis of global earthquake disasters

4.1 Temporal trends of global earthquake disasters

4.1.1 Inter-annual trend analysis of global earthquake disasters

Inter-annual variability in global earthquake disaster impacts from 1980 to 2024 reveals distinct and contrasting trends across different indicators (Figure 1). The number of earthquakes shows a clear upward trend (slope = 0.15), reflecting a gradual increase in event frequency. Cumulative affected population exhibits only a slight upward trend with substantial year-to-year fluctuations, while the average affected population per event shows only a marginal increase over time. The mortality rate displays a mild downward trend, corresponding to a decline in fatalities relative to exposed populations. Cumulative economic losses also show a slight but statistically insignificant upward tendency, whereas average economic loss per event demonstrates a weak declining trend. In contrast, average deaths per event reveal a strong upward trend (slope = 12.73), associated with a limited number of high-impact catastrophic events, while cumulative fatalities fluctuate considerably without a statistically significant long-term trend. Overall, the inter-annual analysis reveals a temporal decoupling between earthquake occurrence and disaster consequences, characterized by increasing event frequency, declining mortality rates, and contrasting behaviors between cumulative and per-event impact indicators.

https://doi.org/10.5194/egusphere-2025-6499
Preprint. Discussion started: 13 January 2026
© Author(s) 2026. CC BY 4.0 License.

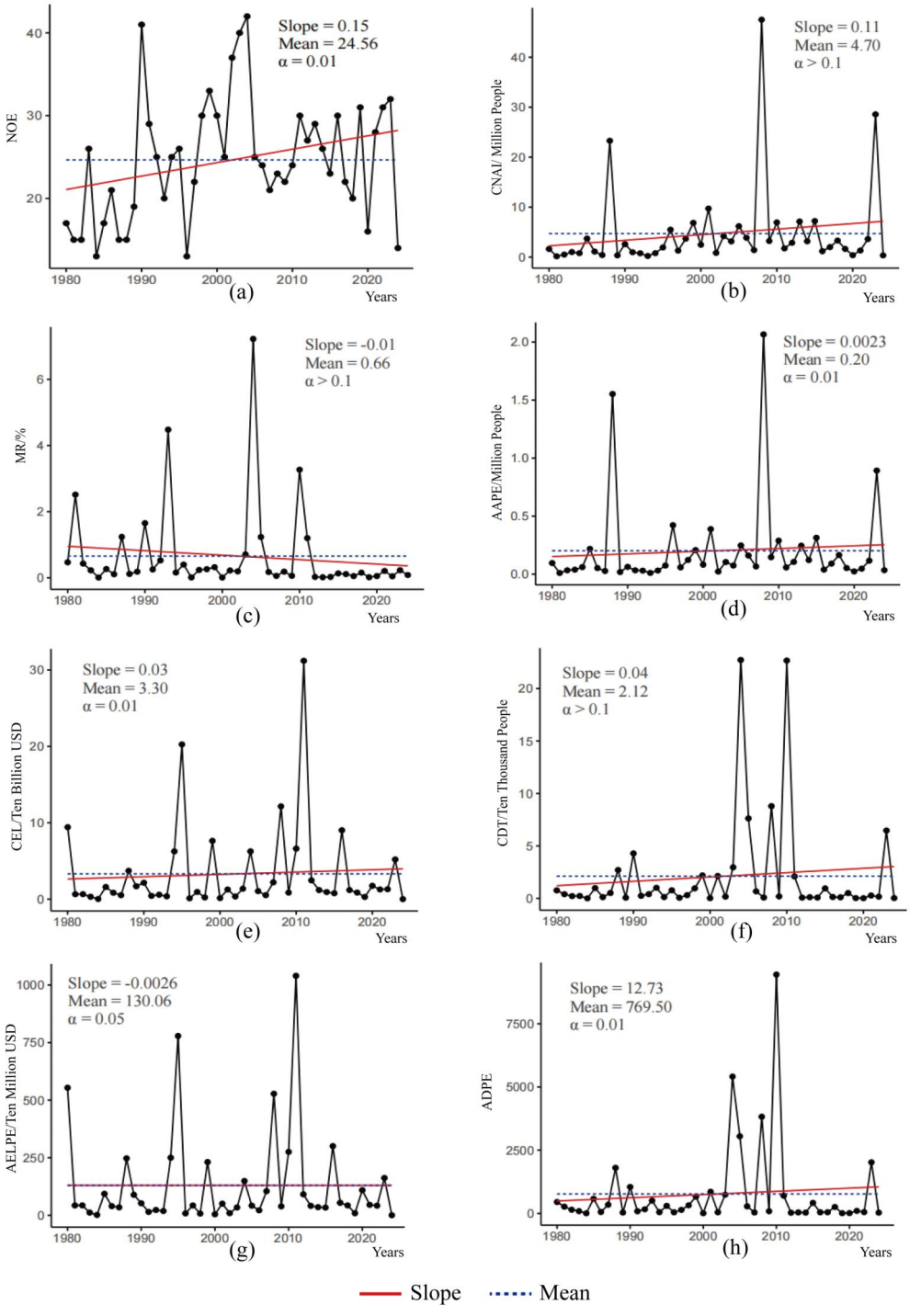

Figure 1. Temporal trends of major global earthquake disaster indicators in 1980-2024. a) Number of Earthquakes; b) Cumulative Number of Affected People ; c) Mortality Rate ; d) Average Number of Affected People per Event; e) Cumulative Economic Losses; f) Cumulative Number of Fatalities; g) Average Economic Loss per Event; h) Average Number of Fatalities per Event.

https://doi.org/10.5194/egusphere-2025-6499
Preprint. Discussion started: 13 January 2026
© Author(s) 2026. CC BY 4.0 License.

4.1.2 Multi-period trend analysis based on three 15-year time windows

To examine longer-term shifts in earthquake disaster impacts, a multi-period trend analysis was conducted using three consecutive 15-year time windows, allowing comparison of disaster severity across different development stages. Eight earthquake disaster indicators were examined across three consecutive 15-year periods (Figure 2). Most indicators—including mortality rate, cumulative deaths, average deaths per event, cumulative affected population, and average affected population per event—reached their highest levels during the second period (1995–2010). In contrast, economic indicators showed a slightly different pattern: although cumulative and per-event economic losses remained high during the third period (2011–2024), their values were slightly lower than those of the second period. Earthquake frequency also increased markedly in the second period and then declined slightly in the third, while remaining above the level observed in the first period. In the most recent period, substantial reductions in cumulative and per-event fatalities and affected populations led to a pronounced decline in mortality rates. These results indicate a recent reduction in the lethality of global earthquake disasters, occurring alongside persistently high—though slightly reduced—levels of economic exposure.

https://doi.org/10.5194/egusphere-2025-6499
Preprint. Discussion started: 13 January 2026
© Author(s) 2026. CC BY 4.0 License.

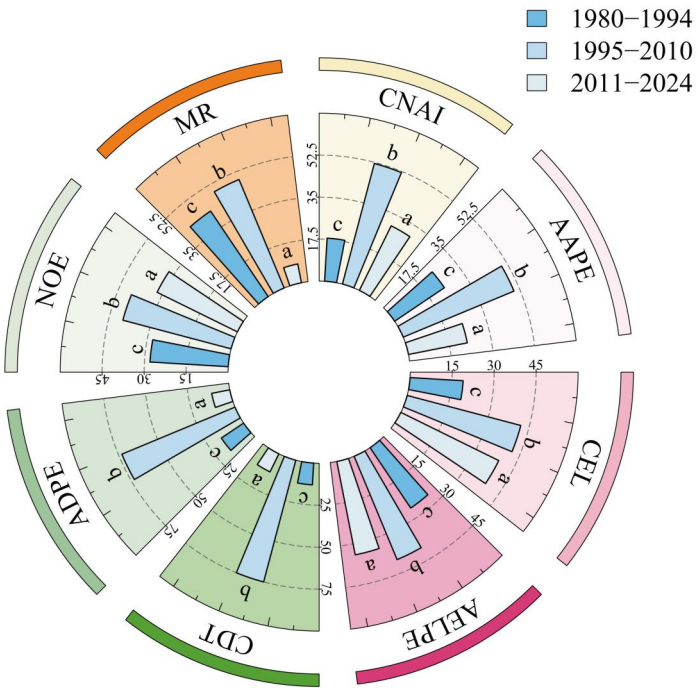

Figure 2. Analysis of changes in global earthquake disaster indicators from 1980 to 2024. NOE represents number of earthquakes, CNAI represents cumulative number of affected people, CEL represents cumulative economic losses, CDT represents cumulative number of fatalities, AAPE represents average number of affected people per event, AELPE represents average economic loss per event, ADPE represents average number of fatalities per event, MR represents mortality rate.

By integrating inter-annual variability with multi-period trend analysis, this section captures both short-term fluctuations and longer-term shifts in global earthquake disaster impacts. These temporal patterns provide a descriptive baseline for interpreting the spatial heterogeneity and associated drivers of earthquake disasters examined in subsequent sections.

4.2 Multi-scale spatial patterns of global major seismic disasters

The spatial distribution of global earthquake disasters is shaped by the combined configuration of tectonic settings, population exposure, and socio-economic conditions, rather than by seismicity alone. To describe spatial heterogeneity in a manner that is comparable across both administrative and geophysical units, the analysis is conducted at three complementary scales. At the continental scale, aggregated indicators provide a first-order overview of where earthquake disaster impacts concentrate globally. At the national scale, spatial mapping and trend testing characterize cross-country differences in disaster impacts and their temporal directions. At the tectonic-plate scale, centroid migration and standard deviation ellipse analyses are used

https://doi.org/10.5194/egusphere-2025-6499
Preprint. Discussion started: 13 January 2026
© Author(s) 2026. CC BY 4.0 License.

to trace the spatial reorganization of earthquake disaster hotspots over time. Together, these analyses describe where disaster impacts are concentrated, how those concentrations shift through time, and how spatial patterns differ across tectonic contexts.

4.2.1 Continental differences of global major seismic disasters

Continental-scale comparison provides a first-order description of spatial heterogeneity in global earthquake disasters, reflecting broad contrasts in tectonic environments, population exposure, and development conditions.. Across 1980-2024, the composition of disaster indicators differs markedly by continent (Figure 3). Asia accounts for the largest shares of most indicators—including earthquake frequency, cumulative affected population, cumulative economic losses, and cumulative fatalities—consistent with the coexistence of extensive seismic belts and large exposed populations.. In contrast, the Americas contribute the largest shares of mortality rate and average deaths per event, indicating that per-event mortality metrics are strongly influenced by a limited number of high-impact catastrophic events.Europe shows comparatively low earthquake frequency but ranks second in average economic loss per event, corresponding to high-value built environments and concentrated economic assets. Africa and Oceania represent small proportions for most indicators; however, Africa exhibits relatively elevated mortality-related shares relative to event counts, implying heightened vulnerability in specific national contexts rather than higher seismic activity.

https://doi.org/10.5194/egusphere-2025-6499
Preprint. Discussion started: 13 January 2026
© Author(s) 2026. CC BY 4.0 License.

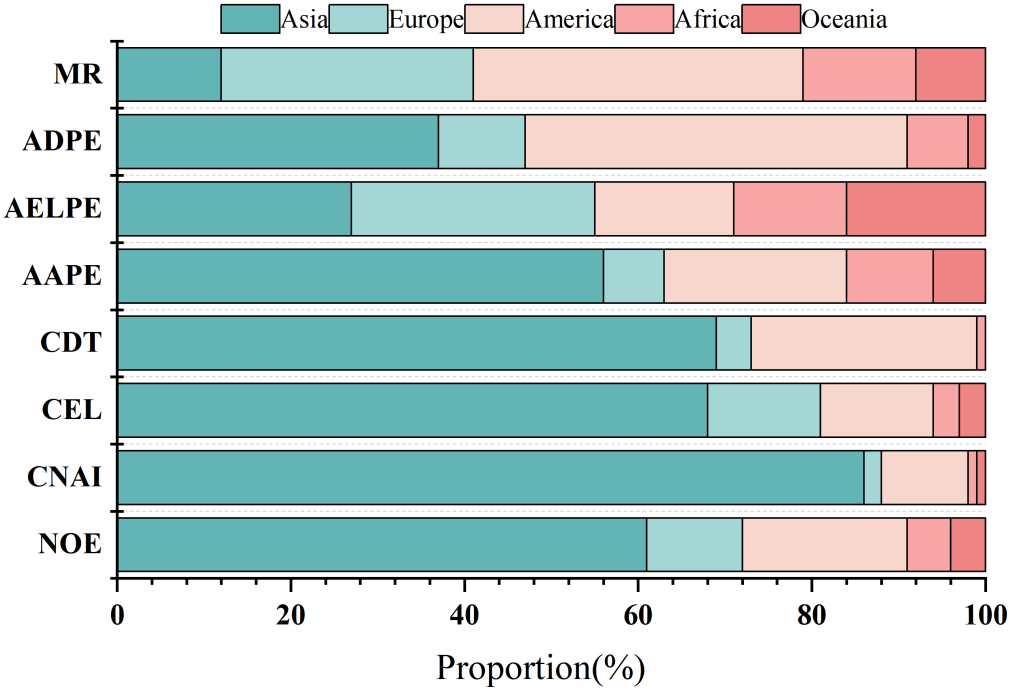

Figure 3. Continental disparities in the composition of global earthquake disaster indicators (1980–2024). NOE represents number of earthquakes, CNAI represents cumulative number of affected people, CEL represents cumulative economic losses, CDT represents cumulative number of fatalities, AAPE represents average number of affected people per event, AELPE represents average economic loss per event, ADPE represents average number of fatalities per event, MR represents mortality rate.

4.2.2 Spatiotemporal variability analysis of global seismic disasters at the national scale

Pronounced spatial differences are observed in the national-level trends of eight seismic disaster indicators during 1980–2024. Seismic frequency (Figure 4.a) exhibits predominantly non-significant temporal variation ($-1.64 \leq Z \leq 1.64$) across most countries, while significant increases ($Z > 1.64$) appear mainly in parts of East and Southeast Asia, where absolute earthquake counts are also high. Significant decreases ($Z < -1.64$) occur sporadically without forming coherent regional clusters. Mortality-related indicators (Figure 4.(b , f)) display widespread significant declines across Asia, Africa, and Oceania, whereas significant upward trends are restricted to a small number of countries in Eastern Europe, Central America, and South Asia. Cumulative and per-event affected populations (Figure 4.(c , d)) show high values in China, India, Indonesia, and parts of South Asia, with significant increases along the western coast of South America, South Asia, and the Indonesian archipelago, while many other regions exhibit non-significant temporal changes. Cumulative fatalities (Figure 4.e) are concentrated in a limited group of countries (e.g., China, India, Iran, Turkey, and Haiti), but trend directions vary, with both increases and decreases observed across different subregions.

https://doi.org/10.5194/egusphere-2025-6499
Preprint. Discussion started: 13 January 2026
© Author(s) 2026. CC BY 4.0 License.

Economic-related indicators demonstrate another layer of spatial heterogeneity. High cumulative economic losses (Figure 4.g) are concentrated in the United States, Japan, China, Italy, and Turkey, with significant upward trends present in East Asia, the Mediterranean region, and parts of South America. By contrast, many countries in Africa, Central Asia, and Eastern Europe show limited or statistically non-significant temporal variation. Average economic loss per event (Figure 4.h) is highest in high-income countries, including Japan, New Zealand, Italy, and the United States, although trend directions vary across national contexts. Overall, national-scale results emphasize that statistically significant trends are spatially clustered for certain indicators—particularly economic losses—whereas non-significant trends dominate large portions of the Global South.

https://doi.org/10.5194/egusphere-2025-6499
Preprint. Discussion started: 13 January 2026
© Author(s) 2026. CC BY 4.0 License.

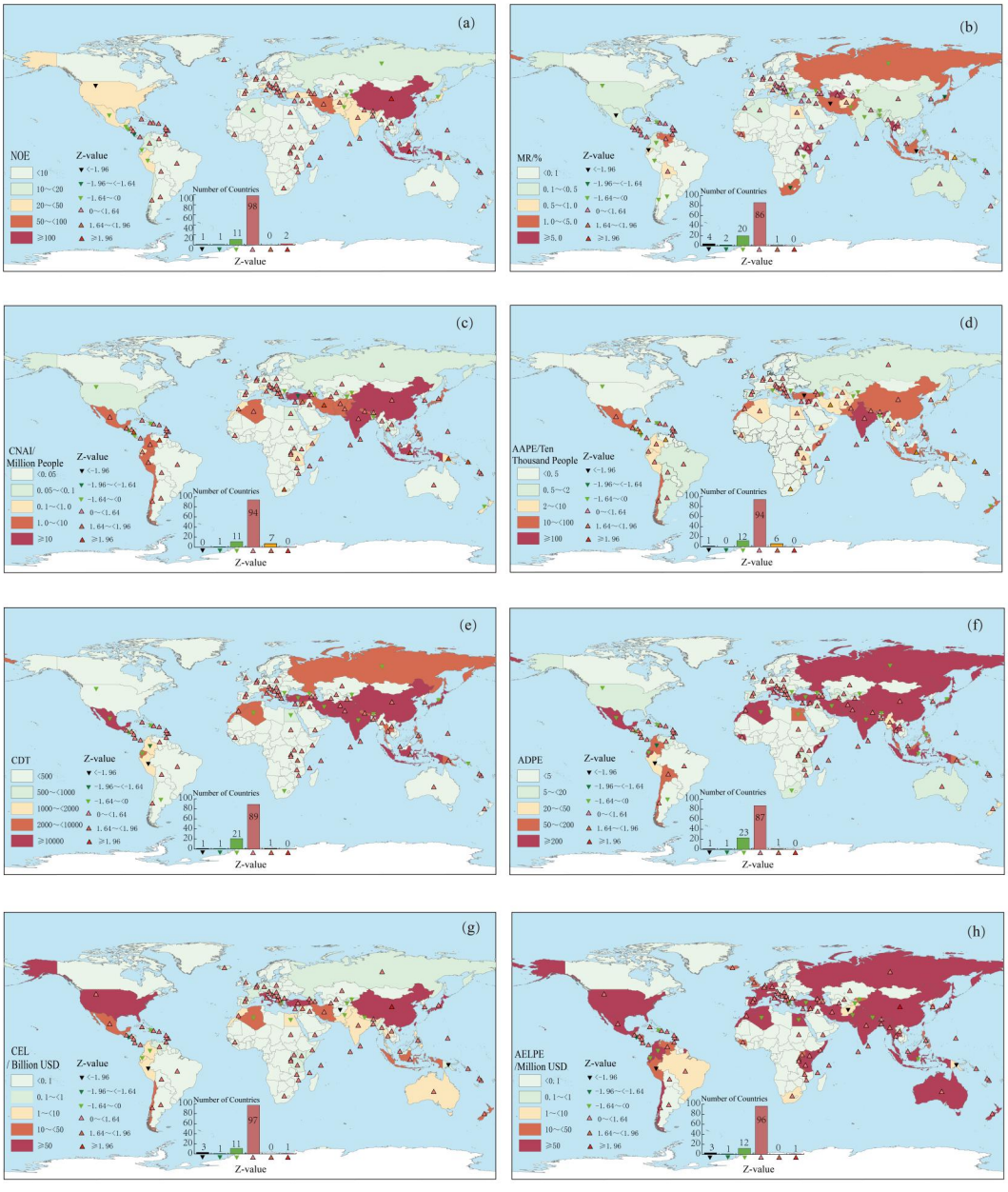

Figure 4. Spatial heterogeneity and temporal trends of eight earthquake disaster indicators at the national scale (1980–2024). a) Earthquake occurrence; b) Mortality rate; c) Cumulative affected population; d) Average affected population per event; e) Cumulative fatalities; f) Average fatalities per event; g) Cumulative economic losses; h) Average economic loss per event.

https://doi.org/10.5194/egusphere-2025-6499
Preprint. Discussion started: 13 January 2026
© Author(s) 2026. CC BY 4.0 License.

4.2.3 Spatiotemporal evolution of global seismic disaster centroids across tectonic plates

The spatial pattern of global seismic disasters exhibits a clear and structured evolution over the period 1980–2024, as reflected by systematic shifts in the geometric centroid and associated dispersion patterns (Figure 5). At the global scale, the centroid trajectory indicates an overall eastward tendency with alternating north–south adjustments, forming a coherent migration path across successive periods.

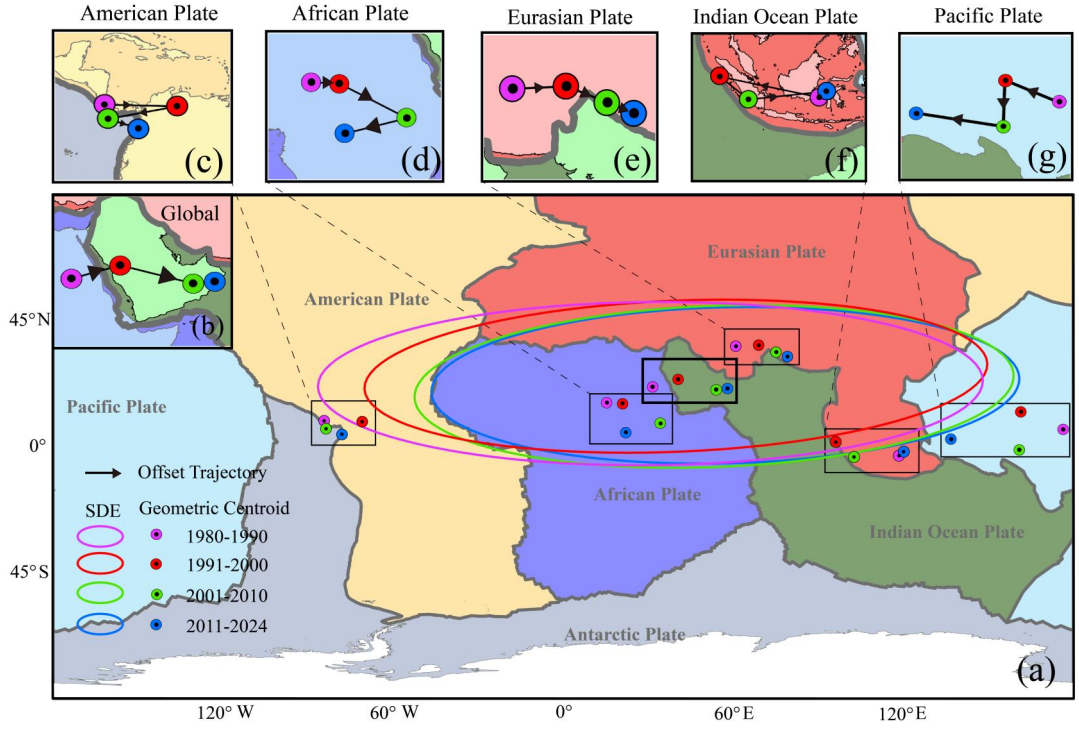

Figure 5. Spatiotemporal evolution of global and plate-scale seismic disaster centroids and spatial dispersion patterns from 1980 to 2024. a) Global standard deviation ellipses and centroid trajectories of seismic disasters across four periods; b) Global centroid displacement trajectory; c) Centroid shifts on the American Plate; Centroid shifts on the d) African Plate, e) Eurasian Plate, f) Indian Ocean Plate, and g) Pacific Plate.

Specifically, the centroid was located in northeastern Africa west of the Red Sea during 1980-1990, shifted northeastward toward the Arabian Peninsula in 1991-2000 (˜909 km), moved southeastward to the central Arabian Peninsula in 2001–2010 (˜1,476 km), and then adjusted northeastward during 2011–2024 (˜433 km) (Table 1). This sequence describes a gradual re-centering of earthquake disaster impacts toward the Middle East–western Indian Ocean region, rather than a shift in seismicity itself. Changes in the spatial dispersion of seismic disasters further support this reorganization. The semi-major axis of the global standard deviation ellipse decreased continuously across periods, indicating a contraction in the longitudinal extent of

https://doi.org/10.5194/egusphere-2025-6499
Preprint. Discussion started: 13 January 2026
© Author(s) 2026. CC BY 4.0 License.

earthquake disaster impact distribution, while changes in the semi-minor axis were smaller and alternated in direction (Table 1). The dominant orientation remained stable across periods, consistent with the alignment of major global seismic belts.

Table 1. Temporal evolution of the location and displacement of the global seismic disaster centroid (1980–2024).

Analysis period	Centroid location	Displacement distance (km)	Dominant shift direction	Change in semi-major axis (km)	Change in semi-minor axis (km)
1980–1990	31.49°E, 21.28°N	–	–	–	–
1991–2000	40.48°E, 23.92°N	908	Northeastward	-732	-217
2001–2010	53.94°E, 20.27°N	1,476	Southeastward	-419	180
2011–2024	57.91°E, 20.68°N	433	Northeastward	-203	-91

At the plate scale, centroid trajectories display pronounced regional heterogeneity (Figure 5.c–g; Table 2). On the American Plate, centroid movements are relatively short and primarily oriented southeastward, corresponding to localized adjustments in the spatial concentration of disaster impacts. The African Plate shows more pronounced centroid displacements, generally trending eastward and southeastward, reflecting its broad spatial extent and dispersed seismic activity. The Eurasian Plate exhibits comparatively limited centroid movement despite its extensive geographic coverage, indicating a spatially expansive but relatively stable impact distribution. In contrast, centroid trajectories on the Indian Ocean and Pacific Plates are more dynamic, with alternating directional shifts concentrated around Southeast Asia, Indonesia, and adjacent subduction zones, highlighting localized but active reorganization of disaster hotspots.

https://doi.org/10.5194/egusphere-2025-6499
Preprint. Discussion started: 13 January 2026
© Author(s) 2026. CC BY 4.0 License.

Table 2. Plate-specific centroid locations, displacement distances, and dominant shift directions of global seismic disasters during 1980–2024.

Tectonic plate	Analysis period	Centroid location	Displacement distance (km)	Dominant shift direction
Pacific Plate	1980–1990	179.26°E, 5.48°N	–	–
	1991–2000	161.43°E, 11.28°N	2039	Northwestward
	2001–2010	161.03°E, 1.60°S	1433	Southwestward
	2011–2024	137.57°E, 1.98°N	2576	Northwestward
Indian Ocean Plate	1980–1990	118.45°E, 3.23°S	–	–
	1991–2000	96.75°E, 1.39°N	2433	Northwestward
	2001–2010	103.00°E, 3.69°S	834	Southeastward
	2011–2024	119.96°E, 1.86°S	1887	Northeastward
Eurasian Plate	1980–1990	61.27°E, 35.30°N	–	–
	1991–2000	69.54°E, 35.69°N	716	Northeastward
	2001–2010	75.86°E, 33.20°N	685	Southeastward
	2011–2024	79.95°E, 31.56°N	458	Southeastward
African Plate	1980–1990	15.77°E, 14.38°N	–	–
	1991–2000	21.33°E, 14.11°N	605	Southeastward
	2001–2010	34.89°E, 6.96°N	1487	Southeastward
	2011–2024	22.57°E, 3.80°N	1385	Southwestward
American Plate	1980–1990	83.67°W, 8.95°N	–	–
	1991–2000	70.13°W, 8.65°N	1477	Southeastward
	2001–2010	82.97°W, 6.12°N	1435	Southwestward
	2011–2024	77.32°W, 4.22°N	658	Southeastward

Overall, the combined global and plate-scale results suggest that global centroid migration is coherent in direction, while the magnitude and orientation of centroid shifts differ across plates, underscoring the role of tectonic context in shaping the spatial reorganization of earthquake disaster impacts.

4.3 Drivers of global earthquake disaster impacts

The temporal and spatial analyses above reveal a clear decoupling between the physical occurrence of earthquakes and the severity of their impacts. While tectonic plate boundaries structure the global pattern of seismicity, earthquake consequences vary substantially across countries even under broadly comparable hazard settings. This spatial heterogeneity indicates that variations in disaster impacts cannot be accounted for by seismicity alone and are closely associated with differences in exposure and vulnerability conditions. Building on the multi-scale patterns identified in Sections 3.1 and 3.2, this subsection

https://doi.org/10.5194/egusphere-2025-6499
Preprint. Discussion started: 13 January 2026
© Author(s) 2026. CC BY 4.0 License.

examines national-scale statistical associations between earthquake mortality and multiple socio-environmental factors the Geographical Detector model. Cumulative fatalities are used as the dependent variable, and explanatory factors (Table 3) are grouped into (i) tectonic–locational context (proximity to plate boundaries), (ii) hydro-climatic and environmental conditions, (iii) socioeconomic development and the built environment, and (iv) governance and health-system capacity (Abatzoglou et al., 2018; World Bank, 2025; Sims et al., 2022; World Health Organization, 2025). The analysis quantifies the degree of spatial correspondence between fatalities and individual factors (q-statistics), as well as the extent to which paired factors jointly enhance spatial differentiation in fatalities. In doing so, we address which factors—and which combinations of factors—are most strongly associated with cross-national disparities in earthquake disaster impacts, rather than attempting to infer causal relationships.

Table 3. Explanatory variables used in the geographical detector analysis of national earthquake fatalities and data sources.

Driver category	Indicator	Data source	Representation
Hydro-climatic and environmental conditions	Precipitation	Terraclimate	Represents hydro-climatic conditions that may influence secondary earthquake hazards such as landslides and debris flows.
Hydro-climatic and environmental conditions	Soil Moisture	Terraclimate	Indicates ground saturation conditions that can amplify slope instability and earthquake-triggered environmental damage.
Tectonic–locational context	Distance from Earthquake to Nearest Plate Boundary	EM-DAT	Serves as a proxy for tectonic exposure and proximity to active seismic sources.
Hydro-climatic and environmental conditions	Diurnal Temperature Variation	C-LSAT	Reflects short-term climatic stress that may affect environmental vulnerability and human health conditions.
Hydro-climatic and environmental conditions	Composite Environmental Quality Index	Figshare	Integrates multiple environmental attributes to characterize overall ecological and land-surface conditions.
Socioeconomic development and the built environment	GDP	Zenodo	Represents national economic development level and the concentration of exposed economic assets.
Socioeconomic development and the built environment	Commercial Facility Density	Figshare	Captures the intensity of economic activity and built-environment concentration.
Socioeconomic development and the built environment	GDP Growth Rate	ESG	Reflects economic dynamics and development trajectories influencing exposure and recovery capacity.
Socioeconomic development and the built environment	Population Density	LandScan	Represents human exposure intensity in seismically active areas.
Socioeconomic development and the built environment	Level of Social Infrastructure	Figshare	Indicates the availability of basic public services and urban support capacity.
Governance and health-system capacity	Government Effectiveness Estimate	ESG	Represents institutional capacity for regulation enforcement, emergency response, and disaster governance.
Governance and health-system capacity	Physicians per 10,000 Population	GHO	Serves as a proxy for health system capacity and post-disaster medical response potential.

https://doi.org/10.5194/egusphere-2025-6499
Preprint. Discussion started: 13 January 2026
© Author(s) 2026. CC BY 4.0 License.

4.3.1 Individual drivers of spatial variation in earthquake mortality

The factor detector results show pronounced spatial heterogeneity in the associations between individual factors and cumulative earthquake fatalities (Figure 6.a). Population density (Factor 1) yields the highest explanatory power ($q = 0.41$), indicating that cross-national differences in exposure are closely aligned with the spatial differentiation of cumulative fatalities at the national scale. Development-related indicators, including GDP (Factor 2; $q = 0.39$) and the level of social infrastructure (Factor 3; $q = 0.36$), also exhibit relatively high explanatory power, suggesting that fatality patterns co-vary with development level and built-environment conditions across countries.

A second group of factors shows moderate explanatory power, including physicians per 10,000 population (Factor 8; $q = 0.21$) and governance-related indicators (Factors 7–9; $0.22 \geq q \geq 0.12$). These results indicate that health-system capacity and institutional conditions are statistically associated with part of the observed spatial differentiation in fatalities. By contrast, the tectonic–locational proxy distance to the nearest plate boundary (Factor 12; $q = 0.05$) shows comparatively low explanatory power when considered alone, implying that proximity to active plate margins has limited ability to differentiate national-level fatality outcomes in isolation.

Overall, the single-factor results indicate that no individual variable fully accounts for the observed spatial heterogeneity in earthquake fatalities. Instead, higher q-values are concentrated among exposure- and development-related indicators, providing a basis for examining whether combinations of factors further strengthen spatial differentiation.

https://doi.org/10.5194/egusphere-2025-6499
Preprint. Discussion started: 13 January 2026
© Author(s) 2026. CC BY 4.0 License.

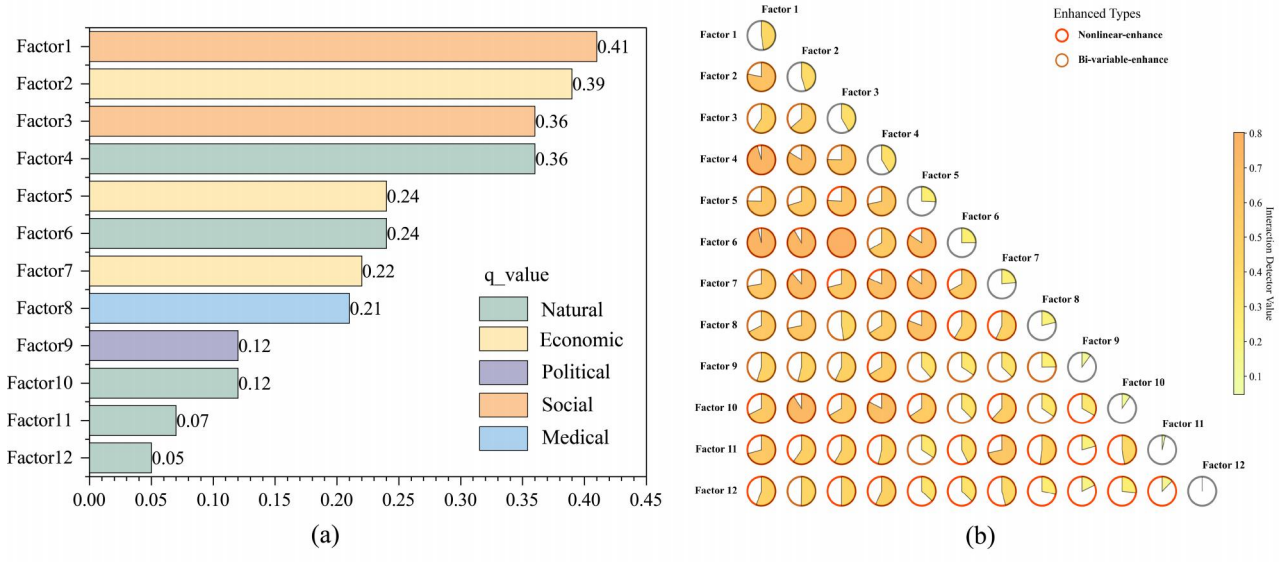

Figure 6. Spatial drivers of cumulative earthquake fatalities and their interaction effects at the global scale. a) Individual explanatory power of drivers based on the factor detector; b) Interaction effects among drivers identified by the interaction detector. Factors include: Factor 1 (Population density); Factor 2 (Gross domestic product (GDP)); Factor 3 (Level of social infrastructure); Factor 4 (Diurnal temperature variation); Factor 5 (Commercial facility density); Factor 6 (Composite environmental quality index); Factor 7 (GDP growth rate); Factor 8 (Physicians per 10,000 population); Factor 9 (Government effectiveness estimate); Factor 10 (Precipitation); Factor 11 (Soil moisture); Factor 12 (Distance to the nearest tectonic plate boundary).

4.3.2 Multi-factor interactions shaping earthquake mortality patterns

Interaction detector results indicate that earthquake fatality patterns are characterized by widespread multi-factor coupling (Figure 6.b). For nearly all factor pairs, joint explanatory power exceeds the corresponding single-factor q-values, and most interactions are classified as bi-variable enhancement or nonlinear enhancement, indicating that spatial differentiation in fatalities strengthens when factors are considered jointly. Interactions that involve high-q exposure and development indicators (e.g., population density with GDP or infrastructure) generally yield stronger joint effects, implying that spatial differentiation in fatalities becomes more pronounced when multiple factors are considered jointly.

Interactions involving high-q exposure and development indicators (e.g., population density combined with GDP or social infrastructure) generally yield stronger joint effects, suggesting that the spatial imprint of exposure is conditioned by national development and capacity contexts. Notably, factors with relatively low independent explanatory power—such as distance to the nearest plate boundary—often exhibit substantially higher explanatory power when combined with exposure- or capacity-related indicators. This pattern suggests that locational hazard context becomes more informative for understanding fatality patterns when evaluated together with where people, assets, and response capacity are distributed.

Overall, the interaction results reinforce that cross-national disparities in earthquake fatalities are associated with overlapping gradients of exposure, development, institutional capacity, and environmental conditions, rather than isolated single drivers.

https://doi.org/10.5194/egusphere-2025-6499
Preprint. Discussion started: 13 January 2026
© Author(s) 2026. CC BY 4.0 License.

4.3.3 A coupled human–environment interpretation of disaster impacts

Taken together, the Geographical Detector results support an interpretation of earthquake disaster impacts as outcomes emerging from the spatial co-location of hazard context, exposure, and vulnerability. Tectonic structures define the global backdrop of seismic hazard, but cross-national variation in fatalities is more strongly aligned with population exposure and differences in development conditions, governance capacity, healthcare availability, and environmental context. The widespread enhancement and frequent nonlinear interactions observed in Figure 6.b further indicate that the association between any single factor and fatalities depends on the configuration of other factors, consistent with a multi-dimensional view of disaster risk.

Importantly, these results describe statistical associations at the national scale and do not imply causal relationships between individual drivers and earthquake fatalities. Nevertheless, they complement the preceding spatiotemporal analyses by clarifying why broadly similar tectonic settings can be associated with markedly different mortality outcomes across countries. In applied terms, the findings suggest that earthquake risk reduction may benefit from integrated intervention strategies that jointly address exposure management and capacity building (e.g., infrastructure and healthcare), rather than relying on single-sector measures. These associations are identified at the national scale and may mask subnational heterogeneity in exposure and vulnerability.

5 Discussion

5.1 Synthesis of key findings

This study provides a multi-scale synthesis of how global earthquake disasters have reorganized in space and time from 1980 to 2024. The temporal analyses reveal a distinct decoupling between seismic occurrence and disaster consequences: although earthquake frequency, human exposure, and cumulative economic losses increased over the study period, mortality rates declined steadily, especially after 2009. Similar findings have been reported globally and regionally, showing that while direct economic losses exhibit significant upward trends, mortality and human vulnerability have generally decreased due to advances in building resilience, governance, and risk management (Daniell et al., 2011; He et al., 2018; Formetta and Feyen, 2019). By integrating long-term interannual trends with period-based comparisons, our results further show that this decoupling varies markedly across regions and national contexts, highlighting the importance of socio-environmental conditions in shaping disaster outcomes. By explicitly combining long-term temporal trends with multi-scale spatial reorganization metrics and interaction-based attribution at the global scale, this study extends existing global earthquake assessments beyond patterns of hazard occurrence toward a comparative understanding of disaster impacts across countries.

Spatial analyses show persistent clustering of seismic disasters along major tectonic boundaries—most prominently the Pacific Ring of Fire and the Alpine–Himalayan belt—yet with strong national-level disparities in disaster severity (Silva et al., 2019). The geometric centroid analysis demonstrates a sustained southeastward migration of global seismic disaster hotspots and a gradual contraction in spatial dispersion. Rather than indicating a shift in seismicity itself, this directional evolution reflects changes in where earthquake impacts concentrate globally. Attribution analysis using the Geographical Detector shows

https://doi.org/10.5194/egusphere-2025-6499
Preprint. Discussion started: 13 January 2026
© Author(s) 2026. CC BY 4.0 License.

that population density, level of public infrastructure, economic level, governance quality, and healthcare capacity, together with their interaction effects, are strongly associated with cross-national variation in earthquake mortality, (Peduzzi, 2019).

These integrated findings illustrate that earthquake disaster outcomes are shaped not only by tectonic processes but also by evolving exposure patterns and socio-environmental vulnerability embedded within human–environment systems (Izquierdo-Horna and Yepez, 2022). Taken together, the spatiotemporal and interaction-based results reinforce the view that global seismic risk manifests through coupled physical and social processes operating across multiple spatial scales.

5.2 Mechanisms behind the spatiotemporal patterns

5.2.1 Tectonic controls on global spatial organization

The concentration of seismic disasters along subduction zones and continental collision belts reflects the fundamental role of lithospheric deformation in structuring global hazard patterns. Subduction zones such as the western Pacific exhibit high strain accumulation and megathrust potential, producing recurrent high-impact events (Silva et al., 2019). Collision zones like the India–Eurasia boundary contribute large, shallow crustal earthquakes affecting densely populated regions. The observed southeastward migration of the global seismic disaster centroid aligns with increasingly active segments of the western Pacific and Southeast Asian tectonic boundaries, consistent with long-term spatial concentration of seismic risk along major plate margins (Peduzzi et al., 2009). Importantly, this migration reflects a redistribution of disaster impacts rather than a systematic change in plate-scale tectonic processes.

5.2.2 Population exposure and socioeconomic vulnerability

National-level disparities arise primarily from differences in exposure and vulnerability rather than differences in seismicity. Rapidly urbanizing, high-density countries—including China, India, and Indonesia—experience large affected populations due to concentrated settlements in seismically active regions (He et al., 2018). Nations with limited governance capacity or weak institutional enforcement, such as Haiti and Nepal, tend to exhibit disproportionate mortality even from moderate events (NicBhloscaidh et al., 2021). Conversely, high-income countries such as Japan, Italy, and the United States incur large economic losses because of high asset concentration and aging infrastructure. Recent social vulnerability assessments confirm that governance quality, healthcare access, and demographic structure significantly shape national earthquake mortality rates (Ma et al., 2023). These contrasts further illustrate how similar hazard contexts may correspond to markedly different disaster outcomes under varying social and institutional conditions.

5.2.3 Divergent trends: declining mortality, rising economic losses

The notable decline in global earthquake mortality suggests steady advances in structural safety, early warning systems, and emergency response capacity (Formetta and Feyen, 2019). However, the simultaneous rise in economic losses reflects intensifying exposure of high-value assets and stronger global economic interdependencies (Daniell et al., 2011). This divergence highlights a core risk paradox: societies have become more capable of protecting lives but remain economically fragile due

https://doi.org/10.5194/egusphere-2025-6499
Preprint. Discussion started: 13 January 2026
© Author(s) 2026. CC BY 4.0 License.

to accumulated development in hazardous areas. Such paradoxes illustrate shifting vulnerabilities within socio-ecological systems and underscore the necessity of integrating social, economic, and physical dimensions of risk (Izquierdo-Horna and Yepez, 2022). Our results indicate that this divergence is spatially uneven, with the strongest contrasts occurring in rapidly urbanizing and economically integrated seismic regions.

5.2.4 Implications for global seismic risk governance

Beyond identifying where seismic hazards are concentrated, the results highlight how disaster impacts emerge from the spatial co-occurrence of tectonic exposure and socio-institutional conditions. Plate-boundary regions require strategies that consider both seismic hazards and potential interactions with climatic extremes such as heavy rainfall–triggered landslides (Cvetković et al., 2024). Rapidly urbanizing regions should target improvements in land-use planning, building quality, and emergency resource allocation to reduce both human and economic impacts. In countries facing governance challenges, enhancing institutional capacity, healthcare access, and political stability is essential for reducing future mortality (Peduzzi, 2019). More broadly, the findings underscore the importance of multi-scale disaster risk governance frameworks that integrate tectonic exposure, development trajectories, and social vulnerability. By identifying locations where high seismic exposure coincides with elevated socio-environmental vulnerability, this study provides a spatially explicit basis for prioritizing disaster risk reduction and resilience-building efforts across scales.

5.2.5 Limitations

Several limitations should be acknowledged. EM-DAT underreports small and moderate events, which may affect frequency-related indicators (Cvetković et al., 2024). National-scale spatial analysis simplifies complex local fault geometries and intra-country heterogeneity. Geographical Detector identifies spatially stratified associations but cannot determine causal direction (Peduzzi, 2019). Additionally, socioeconomic variables are often static or infrequently updated, limiting the ability to model rapid socio-economic transitions.

5.2.6 Future research directions

Future work should incorporate near–real-time seismic and socio-environmental data, develop dynamic models to track evolving risk landscapes, and examine compound hazards involving interactions between seismic activity and climatic extremes. Integrating machine learning with physical models may further enhance predictive capability (Silva et al., 2019). Expanding high-resolution exposure and vulnerability datasets will support more detailed subnational risk assessments (Ma et al., 2023). Ultimately, advancing global earthquake risk research will require closer integration of physical seismology, spatial analysis, and socio-institutional vulnerability studies, in order to better support disaster risk reduction and resilience planning. The analytical framework adopted here demonstrates how global disaster databases can be combined with spatial reorganization and interaction analyses to inform comparative risk assessment and policy-relevant interpretation.

https://doi.org/10.5194/egusphere-2025-6499
Preprint. Discussion started: 13 January 2026
© Author(s) 2026. CC BY 4.0 License.

6 Conclusions

This study analyzed the spatiotemporal evolution of global earthquake disasters from 1980 to 2024 and examined national-scale factors associated with cross-country differences in disaster impacts. By integrating long-term temporal analysis, multi-scale spatial assessment, centroid-based spatial metrics, and factor interaction analysis, the study addresses four interrelated research questions.

First, with respect to long-term temporal change, global earthquake disasters exhibit a persistent decoupling between occurrence and consequences. While earthquake frequency, affected population, and cumulative economic losses increased overall, mortality rates declined substantially after the early 2000s, reflecting an overall improvement in life protection relative to growing exposure rather than a reduction in hazard occurrence.

Second, in terms of spatial heterogeneity, earthquake disaster impacts are unevenly distributed across continents and countries. Asia accounts for a large share of global earthquake disasters in terms of frequency, affected population, fatalities, and economic losses, yet the severity of impacts differs markedly among countries, indicating that broadly comparable tectonic settings are associated with highly divergent disaster outcomes.

Third, regarding spatial reorganization, the centroid of earthquake disaster impacts shows a systematic eastward to southeastward shift over the study period, while the standard deviation ellipse indicates a relatively stable orientation accompanied by a modest contraction in spatial dispersion. Plate-level comparisons further reveal differentiated centroid trajectories across major tectonic plates, which is consistent with a long-term re-centering of global disaster impacts rather than changes in underlying seismic processes.

Finally, with respect to spatial disparities in fatalities, the Geographical Detector results indicate that population density and development-related factors exhibit relatively strong explanatory power. More importantly, interactions among socioeconomic, governance, health, environmental, and hazard-related variables consistently enhance explanatory strength beyond single-factor effects, highlighting that observed fatality patterns are statistically associated with coupled natural–social conditions rather than with tectonic context alone.

Overall, the findings underscore that global earthquake disaster impacts are shaped by the spatial convergence of hazard exposure, development pathways, and institutional capacity. By identifying where disaster impacts diverge under similar hazard conditions and how multiple factors co-vary spatially, this study provides comparative, globally consistent evidence that can inform risk assessment, preparedness planning, and resilience-oriented decision-making, particularly in regions experiencing rapid exposure growth alongside persistent social and institutional vulnerability.

Data availability

The earthquake disaster data used in this study are derived from the Emergency Events Database (EM-DAT), which is publicly available. Socio-environmental and governance datasets were obtained from openly accessible international databases, as described in the Methods section. The processed datasets and analysis scripts supporting the findings of this study are available from the corresponding author upon reasonable request.

https://doi.org/10.5194/egusphere-2025-6499
Preprint. Discussion started: 13 January 2026
© Author(s) 2026. CC BY 4.0 License.

Author contribution

Z.Z.: Visualization, Writing - Original Draft; **Y.Q.:** Formal Analysis; **Y.Y.:** Writing - Review & Editing; **C.X.:** Visualization. All authors have read and agreed to the published version of the manuscript.

Competing interests

The authors declare that they have no competing interests.

https://doi.org/10.5194/egusphere-2025-6499
Preprint. Discussion started: 13 January 2026
© Author(s) 2026. CC BY 4.0 License.

References

Abatzoglou, J. T., Dobrowski, S. Z., Parks, S. A., and Hegewisch, K. C.: TerraClimate, a high-resolution global dataset of monthly climate and climatic water balance from 1958–2015, Scientific Data, 5, 170 191, https://doi.org/https://doi.org/10.1038/sdata.2017.191, 2018.

Aksha, S. K. and Khanal, S.: An analysis of social vulnerability to natural hazards in Nepal, International Journal of Disaster Risk Science, 10, 310–324, https://doi.org/https://doi.org/10.1007/s13753-018-0192-7, 2019.

Anbarci, N., Escaleras, M., and Register, C. A.: Earthquake fatalities: The interaction of nature and political economy, Journal of Public Economics, 89, 1907–1933, https://doi.org/https://doi.org/10.1016/j.jpubeco.2004.08.002, 2005.

Ansari, A., Al-Awadhi, T., Al-Rawas, G., and Al-Busaidi, A.: Integrated GIS–AHP based assessment of earthquake vulnerability and risk in residential areas of Al-Seeb, Muscat Governorate (Oman), Scientific Reports, 15, 17 618, https://doi.org/https://doi.org/10.1038/s41598-025-17618-6, 2025.

Bird, P.: An updated digital model of plate boundaries, Geochemistry, Geophysics, Geosystems, 4, 1027, https://doi.org/https://doi.org/10.1029/2001gc000252, 2003a.

Bird, P.: PB2002: Plate Boundary and Tectonic Data (2003) [dataset], 2003b.

Burton, I.: Understanding risk in a changing world, Natural Hazards, 78, 1951–1968, https://doi.org/https://doi.org/10.1007/s11069-015-1950-3, 2015.

Cannon, S. H., Ellen, S. D., and Wieczorek, G. F.: Landslide hazard associated with earthquakes: A global review, Engineering Geology, 70, 1–15, https://doi.org/https://doi.org/10.1016/S0013-7952(03)00057-2, 2003.

Casella, G. and Berger, R. L.: Statistical Inference, Duxbury Press, Pacific Grove, CA, 2002.

Cohen, M. and Werker, E.: The political economy of "natural" disasters, Journal of Conflict Resolution, 52, 795–819, https://doi.org/https://doi.org/10.1177/0022002708321421, 2008.

CRED: EM-DAT - The International Disaster Database (2024) [dataset], 2024.

Cutter, S. L.: Facing global environmental change: Piecing together the human exposure mosaic, Annals of the American Association of Geographers, 111, 897–903, https://doi.org/https://doi.org/10.1080/24694452.2021.1881107, 2021.

Cvetković, V. M., Renner, R., Aleksova, B., and Lukić, T.: Geospatial and Temporal Patterns of Natural and Man-Made (Technological) Disasters (1900–2024): Insights from Different Socio-Economic and Demographic Perspectives, Applied Sciences, 14, 8129, 2024.

Daniell, J. E., Khazai, B., Wenzel, F., and Vervaeck, A.: The CATDAT damaging earthquakes database, Nat. Hazards Earth Syst. Sci., 11, 2235–2251, https://doi.org/https://doi.org/10.5194/nhess-11-2235-2011, 2011.

Daniell, J. E., Vervaeck, A., Wenzel, F., and Khazai, B.: The worldwide economic impact of earthquake disasters, International Journal of Disaster Risk Reduction, 21, 261–271, https://doi.org/https://doi.org/10.1016/j.ijdrr.2016.11.002, 2017.

De Ruiter, M. C., Couasnon, A., Ward, P. J., Daniell, J. E., and Aerts, J. C. J. H.: The asynergies of structural disaster risk reduction: Building-level DRR measures for earthquake vs flood vulnerability, Earth's Future, 9, e2020EF001 531, https://doi.org/https://doi.org/10.1029/2020ef001531, 2021.

Düzgün, H. Ş., Güney, A. B., Özkan, O., and Taşeli, B. B.: A spatial framework for assessing urban earthquake vulnerability, Natural Hazards, 117, 891–908, https://doi.org/10.1007/s11069-023-05841-8, 2023.

Escaleras, M., Anbarci, N., and Register, C. A.: Public sector corruption and major earthquakes: A potentially deadly interaction, Public Choice, 132, 209–230, https://doi.org/https://doi.org/10.1007/s11127-007-9148-y, 2007.

https://doi.org/10.5194/egusphere-2025-6499
Preprint. Discussion started: 13 January 2026
© Author(s) 2026. CC BY 4.0 License.

Flanagan, B. E., Gregory, E. W., Hallisey, E. J., Heitgerd, J. L., and Lewis, B.: A social vulnerability index for disaster management, Journal of Homeland Security and Emergency Management, 8, Article 3, https://doi.org/https://doi.org/10.2202/1547-7355.1792, 2011.

Formetta, G. and Feyen, L.: Empirical evidence of declining global vulnerability to climate-related hazards, Global Environmental Change, 57, 101 920, https://doi.org/https://doi.org/10.1016/j.gloenvcha.2019.05.004, 2019.

Gall, M., Borden, K. A., and Cutter, S. L.: When do losses count? Six fallacies of natural hazards loss data, Bulletin of the American Meteorological Society, 92, 835–840, https://doi.org/https://doi.org/10.1175/2010bams3090.1, 2011.

Guo, X., Xu, Y., and Li, H.: Assessing social vulnerability to earthquake disaster using county-level data: A case study in Hanzhong City, China, International Journal of Disaster Risk Reduction, 49, 101 632, https://doi.org/https://doi.org/10.1016/j.ijdrr.2020.101632, 2020.

He, X., Wu, J., Wang, C., and Ye, M.: Historical Earthquakes and Their Socioeconomic Consequences in China: 1950–2017, Int J Environ Res Public Health, 15, https://doi.org/10.3390/ijerph15122728, 2018.

Hu, Y., Wang, J., Li, X., Ren, D., and Zhu, J.: Geographical detector-based risk assessment of under-five mortality in the 2008 Wenchuan Earthquake, China, PLoS ONE, 6, e21 427, https://doi.org/https://doi.org/10.1371/journal.pone.0021427, 2011.

Ismail-Zadeh, A.: Earthquakes yes, disasters no, npj Natural Hazards, 1, Article 46, https://doi.org/https://doi.org/10.1038/s44304-024-00049-0, 2024.

Izquierdo-Horna, L. and Yepez, Y.: Dimensions of seismic vulnerability and resilience: A review, International Journal of Disaster Risk Reduction, 68, 102 737, https://doi.org/https://doi.org/10.1016/j.ijdrr.2021.102737, 2022.

Kagan, Y. Y. and Jackson, D. D.: Global earthquake forecasting: Seismicity models and hazard assessment, Annual Review of Earth and Planetary Sciences, 44, 109–137, https://doi.org/https://doi.org/10.1146/annurev-earth-060115-012225, 2016.

Keefer, P., Neumayer, E., and Plümper, T.: Earthquake propensity and the politics of mortality prevention, World Development, 39, 1530–1541, https://doi.org/https://doi.org/10.1016/j.worlddev.2011.03.006, 2011.

Lapietra, I., Bonasia, M., and Pelligra, V.: Unveiling social vulnerability to natural hazards in the European Economic Area, International Journal of Disaster Risk Reduction, 102, 103 651, https://doi.org/https://doi.org/10.1016/j.ijdrr.2023.103651, 2024.

Lee, S., Dodge, J., and Chen, G.: The cost of social vulnerability: An integrative conceptual framework for assessing financial risks in natural disasters, Natural Hazards, 114, 691–712, https://doi.org/https://doi.org/10.1007/s11069-022-05408-6, 2022.

Li, Y., Zhou, Y., and Wang, L.: Impact of economic development levels on the mortality rates of Asian earthquakes, International Journal of Disaster Risk Reduction, 62, 102 409, https://doi.org/https://doi.org/10.1016/j.ijdrr.2021.102409, 2021.

Ma, M., Zhang, Y., Wang, J., and Liu, H.: Spatial assessment of social vulnerability to earthquakes using multi-criteria decision analysis, Scientific Reports, 13, 21 489, https://doi.org/https://doi.org/10.1038/s41598-023-48430-4, 2023.

NicBhloscaidh, M., McCloskey, J., Pelling, M., and Naylor, M.: Do social adaptations increase earthquake resilience?, International Journal of Disaster Risk Reduction, 52, 101 972, https://doi.org/https://doi.org/10.1016/j.ijdrr.2020.101972, 2021.

Noy, I.: The economics of natural disasters: A survey, International Review of Environmental and Resource Economics, 9, 71–108, https://doi.org/https://doi.org/10.1561/101.00000068, 2016.

Peduzzi, P.: Drivers of risk: Exposure, vulnerability and hazard, Progress in Disaster Science, 2, 100 030, https://doi.org/https://doi.org/10.1016/j.pdisas.2019.100030, 2019.

Peduzzi, P. and Herold, H. D. C.: Mapping Disastrous Natural Hazards Using Global Datasets, Natural Hazards, 35, 265–289, https://doi.org/https://doi.org/10.1007/s11069-004-5703-8, 2005.

Peduzzi, P., Dao, H., Herold, C., and Mouton, F.: Assessing global exposure and vulnerability towards natural hazards: the Disaster Risk Index, Nat. Hazards Earth Syst. Sci., 9, 1149–1159, https://doi.org/https://doi.org/10.5194/nhess-9-1149-2009, 2009.

https://doi.org/10.5194/egusphere-2025-6499
Preprint. Discussion started: 13 January 2026
© Author(s) 2026. CC BY 4.0 License.

Reid, P.: Disasters and social inequalities, Sociology Compass, 7, 878–894, https://doi.org/https://doi.org/10.1111/soc4.12080, 2013.

Resource and Environmental Science Data Platform: Resource and Environmental Science Data Platform, https://www.resdc.cn/, last access: 2024/11/10, 2024.

Rosvold, E. L. and Buhaug, H.: GDIS, a global dataset of geocoded disaster locations, Scientific Data, 8, 61, https://doi.org/https://doi.org/10.1038/s41597-021-00846-6, 2021.

Silva, V., Amo-Oduro, D., Calderon, A., Costa, C., Dabbeek, J., Despotaki, V., Martins, L., Pagani, M., Rao, A., Simionato, M., Vigano, D., Yepes-Estrada, C., and Crowley, H.: Assessing seismic hazard and risk globally for an earthquake resilient world, United Nations Office for Disaster Risk Reduction (UNDRR), Contributing Paper to GAR 2019, 2019.

Sims, K., Reith, A., Bright, E., McKee, J., and Rose, A.: LandScan Global 2021 (2021), Oak Ridge National Laboratory [dataset], https://doi.org/10.48690/1527702, 2022.

United Nations Office for Disaster Risk Reduction (UNDRR): Global Assessment Report on Disaster Risk Reduction 2023 (GAR2023), 2023.

Wang, J. F., Li, X. H., Christakos, G., Liao, Y. L., Zhang, T., Gu, X., and Zheng, X. Y.: Geographical detectors-based health risk assessment and its application in the neural tube defects study of the Heshun region, China, International Journal of Geographical Information Science, 24, 107–127, https://doi.org/https://doi.org/10.1080/13658810802443457, 2010.

Wang, J. F., Zhang, T. L., and Fu, B. J.: A measure of spatial stratified heterogeneity, Ecological Indicators, 67, 250–256, https://doi.org/https://doi.org/10.1016/j.ecolind.2016.02.052, 2016.

Wang, X., Xia, J., Dong, B., Zhou, M., and Deng, S.: Spatiotemporal distribution of flood disasters in Asia and influencing factors in 1980–2019, Natural Hazards, 108, 2721–2738, https://doi.org/https://doi.org/10.1007/s11069-021-04798-3, 2021.

World Bank: Environment, Social and Governance (ESG) Data, https://databank.worldbank.org/source/environment-social-and-governance-(esg)-data, last accessed: 2025/7/22, 2025.

World Health Organization: Global Healthcare Statistics 2025, https://www.who.int/data/gho/whs-annex/, last access: 2025/7/22, 2025.

Wu, S., Hu, Z., Wang, Z., Cao, S., Yang, Y., Qu, X., and Zhao, W.: Spatiotemporal variations in extreme precipitation on the middle and lower reaches of the Yangtze River Basin (1970–2018), Quaternary International, 592, 80–96, https://doi.org/https://doi.org/10.1016/j.quaint.2021.04.010, 2021.

Wyss, M., Speiser, M., and Tolis, S.: Earthquake fatalities and potency, Natural Hazards, 119, 1091–1106, https://doi.org/https://doi.org/10.1007/s11069-022-05627-x, 2023.

Xiong, J., Li, J., Cheng, W., Zhou, C., Guo, L., Zhang, X., Wang, N., and Li, W.: Spatial-temporal distribution and the influencing factors of mountain flood disaster in southwest China, Acta Geographica Sinica, 74, 1374–1391, https://doi.org/https://doi.org/10.11821/dlxb201907008, 2019.

Xofi, M., Gkimisi, A., and Karatza, M.: Exposure and physical vulnerability indicators to assess seismic risk, GeoRisk: Assessment and Management of Risk for Engineered Systems and Geohazards, 16, 209–226, https://doi.org/https://doi.org/10.1080/19475705.2022.2068457, 2022.

Zaliapin, I. and Ben-Zion, Y.: Earthquake clusters in Southern California I: Identification and stability, Journal of Geophysical Research: Solid Earth, 118, https://doi.org/https://doi.org/10.1002/jgrb.50179, 2013.